Strengthening of prestressed concrete hollow-core slab openings using near-surface-mounted carbon-fiber-reinforced polymer reinforcement

Karam Mahmoud, Steven Foubert, and Ehab El-Salakawy

- The effect of openings on the behavior of prestressed hollow-core slabs and the efficiency of near-surface-mounted reinforcement as a strengthening technique are investigated.
- Test results showed that the presence of an opening along the flexure span or the shear span significantly decreased the postcracking flexural stiffness and capacity of the slab.
- Strengthening openings with near-surface-mounted carbon-fiber-reinforced polymer strips effectively enhanced the postcracking stiffness, increased the ductility of the member, restored the flexural strength deficit due to cutting the openings, and provided a net increase in flexural capacity.

Precast, prestressed concrete hollow-core slabs are used in many structures, such as commercial and industrial buildings and parking structures. It is common for such structures to undergo changes while still in service, which may result in a reduction in their strength or require them to resist additional loads. One such change is the addition of openings at different locations within the slab span to accommodate intake/exhaust ducts along industrial building roofs or utility conduits along parking structure floors. In such cases, different strengthening techniques can be employed to restore or to enhance the performance of the original structure.

The near-surface-mounted strengthening technique using fiber-reinforced polymer (FRP) composites has proved to be effective for strengthening reinforced concrete structures.[1–14] The noncorrodible, durable nature of FRP composites can successfully mitigate the effects of inclement conditions and effectively improve the structure's performance. Extensive research has been conducted to investigate the behavior of near-surface-mounted strengthened reinforced concrete members.[1–4] These studies aimed to evaluate the feasibility of the near-surface-mounted technique and the bond between the FRP laminates, the surrounding adhesive matrix, and the concrete substrate. Physical and mechanical properties that affect bond performance include concrete strength, type, amount and arrangement of internal and external reinforcement, groove size, groove spacing, edge distance, bonded length, and adhesive material.[5] The near-surface-mounted strength-

ening technique has many advantages over the externally bonded reinforcement strengthening technique, including its more efficient use of FRP material because high tensile stress can be applied to the FRP due to the lower risk of debonding failure and better protection of FRP material from external sources of damage. Moreover, in terms of the capacity of the near-surface-mounted strengthened members, it was found that the linear-elastic behavior of FRP materials allows a strengthened member to carry additional loads even after the internal steel has reached the yielding point.[2,6–10] Unstrengthened members experience increased deformation without an increase in load-carrying capacity once the internal reinforcement begins to yield; this is known as the yielding plateau. However, the stiffening effect provided by the FRP reinforcement provides a linear load-carrying capacity until failure of the composite section.

The behavior of one-way and two-way reinforced concrete slabs with openings strengthened with FRP materials has been previously studied.[11–14] Either externally bonded laminates or near-surface-mounted strips were used to strengthen these slabs. It was found that providing carbon-fiber-reinforced polymer (CFRP) strengthening for slabs with openings effectively enhanced the stiffness and the ultimate load capacity of the slab, where behavior comparable to that of the control slab was observed. Alternatively, the CFRP-strengthened slabs exhibited brittle failure, in contrast to the more ductile behavior of their unstrengthened counterparts.[14] It was also reported that all slabs with CFRP-strengthened openings exhibited an increased load-carrying capacity compared with their counterparts without strengthening.[11] Moreover, a slab with an opening strengthened with near-surface-mounted CFRP strips reached 92% of the slab capacity (compared with 82% for a slab with an unstrengthened opening); however, the near-surface-mounted strips were ineffective in restoring the stiffness of the slab.[12]

This study represents an attempt to investigate the behavior of prestressed hollow-core slabs with either unstrengthened openings or openings strengthened with near-surface-mounted CFRP strips.

Experimental program

The specimens were constructed by a local precast concrete supplier. To replicate the quality of materials used in local construction projects, no modifications were made to the concrete, formwork, high-strength steel, or methods of prestressing. The slabs were cast using zero-slump concrete covered with an insulated tarp and steam cured for 18 hours until the concrete could effectively support the applied prestressing force. After the application of the prestressing forces, the slabs were cut to the specified length and moved to the laboratory for testing.

Test specimens

A total of five prestressed hollow-core slabs were tested to failure. The slabs were 5000 mm (200 in.) long and 203 mm (7.99 in.) thick with a concrete cross-sectional area of 140,194 mm^2 (217.301 in.^{2}). The slabs originally had an internal prestressing steel reinforcement ratio of 0.00274. The prestressing reinforcement consisted of seven size 9 (0.375 in.) strands. In two of the slabs, an opening was cut within the flexural span to reduce the compression area and interrupt a pretensioned strand, which was expected to reduce the flexural capacity by a not-yet-determined amount. In addition, in two other slabs, an opening was cut in the shear span to reduce the web width and to interrupt the middle strand, which could adversely affect the shear capacity of the slab and possibly change the mode of failure. The fifth slab had no opening to serve as a reference. For each opening location, one slab was strengthened with the near-surface-mounted technique.

The opening had a rectangular shape measuring 308 mm (12.1 in.) wide × 600 mm (24 in.) long, $0.25b \times 0.5b$, where b is the width of the hollow-core slab element. The opening locations along the slab profile were dictated by several design constraints, namely mechanical unit specifications, functionality obstructions, and flexure or shear capacity constraints. The middle strand was cut in the slabs with openings. The naming convention of the slabs is as follows:

- The first two letters refer to the presence and location of the opening, so NO, FO, and SO refer to no opening, opening in flexural span, and opening in shear span, respectively.
- The last letter refers to the strengthening using CFRP strips: O for none and S for strengthened.

Table 1 and **Fig. 1** show details of the test slabs.

Materials

Normalweight, high-strength concrete with a target compressive strength of 28 MPa (4100 psi) at 18 hours and 45 MPa (6500 psi) at 28 days was used to cast the specimens. Table 1 gives the compressive strength for each slab on the day of testing. The internal reinforcement used to prestress the slabs was Grade 1860 (Grade 270), seven-wire, low-relaxation, high-strength steel strand. The strands were anchored from one end of the 80 m (260 ft) precasting bed and stressed from the other end. Each seven-wire strand was tensioned individually, beginning with the center strand and moving symmetrically outward. The strands were initially stressed to $0.75f_{pu}$, where f_{pu} is the specified tensile strength of the prestressed steel tendon. The stress in the steel for a given applied load was approximated from the Ramberg-Osgood function as provided in the *CPCI Design Manual*.[15]

Table 1. Details of test specimens

Specimen	Concrete strength, MPa	Internal reinforcement			Opening location	CFRP laminates
		Configuration	Area, mm²	Ratio		
NO-O	64.0	Seven no. 9	383.6	0.00274	None	None
FO-O	64.0	Seven no. 9	383.6	0.00274	Flexure span	None
FO-S	56.5	Seven no. 9	383.6	0.00274	Flexure span	Yes
SO-O	56.5	Seven no. 9	383.6	0.00274	Shear span	None
SO-S	56.5	Seven no. 9	383.6	0.00274	Shear span	Yes

Note: CFRP = carbon-fiber-reinforced polymer; FO-O = slab with flexural span opening; FO-S = slab with flexural span opening strengthened with CFRP strips; NO-O = reference slab with no opening; SO-O = slab with shear span opening; SO-S = slab with shear span opening strengthened with CFRP strips. No. 9 = 29M; 1 mm² = 0.00155 in.²; 1 MPa = 0.145 ksi;

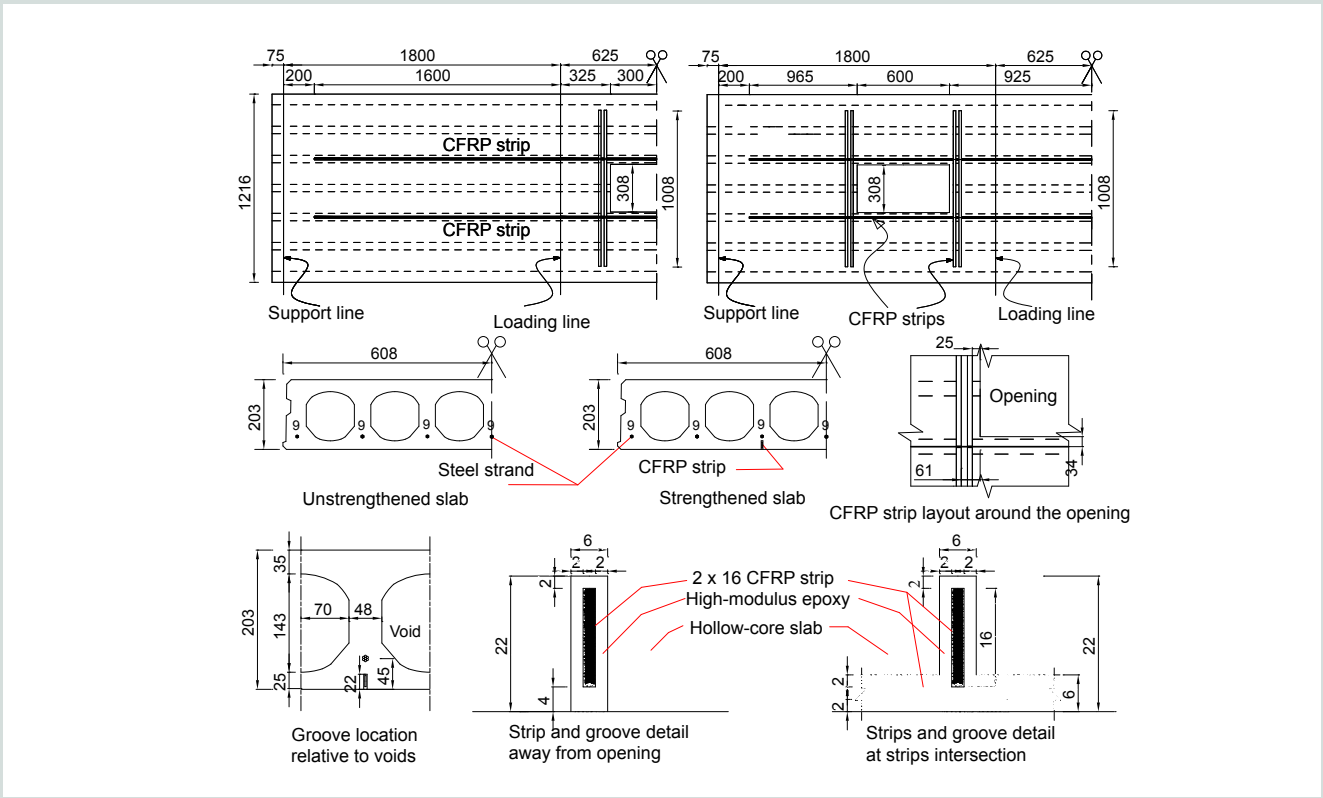

Figure 1. Details and cross section of test slabs and groove details near the voids. Note: CFRP = carbon-fiber-reinforced polymer. All dimensions are in millimeters. 1 mm = 0.0394 in.

The CFRP strips used were 2 mm (0.08 in.) thick and 16 mm (0.63 in.) wide with a nominal area of 32 mm² (0.050 in.²). Based on a standard tensile test performed by the manufacturer, the laminates had a guaranteed modulus of elasticity of 131 GPa (19.0 ksi) and a guaranteed tensile strength of 2068 MPa (300.0 ksi). The guaranteed modulus of elasticity is equal to the mean value, while the guaranteed tensile strength is equal to the mean tensile strength minus three times the standard deviation. The structural adhesive used to bond the near-surface-mounted CFRP laminates to the concrete substrate had a tensile strength of 62 MPa (9.0 ksi) and a flexural modulus of 3792 MPa (550.0 ksi).

Cutting openings and strengthening procedure

A handheld concrete saw was used to cut the openings and the longitudinal grooves along the soffits of the slabs. The longitudinal grooves were terminated 200 mm (8 in.) from each support, superseding the development length required past the maximum moment region. The target depth of the groove was 22 mm (0.87 in.) with a thickness of 6 mm (0.2 in.) to allow 2 mm (0.08 in.) of epoxy cover on each side of the strip. Because the longitudinal and transverse strips intersected, it was not possible for them to have the same orientation without interruption. Therefore,

the transverse strips were installed in grooves oriented as shown in Fig. 1. After the grooves were cut, the structural adhesive was injected along the grooves using specialized mixing and dispensing equipment. Epoxy was applied until the groove was ¾ full, leaving adequate space for the CFRP laminate. The strips were then pushed into the grooves in the required orientation. After installation of the near-surface-mounted system in specimens FO-S and SO-S, they were kept in normal laboratory conditions for at least one week prior to testing.

Test setup and instrumentation

The slabs were subjected to a four-point bending scheme to failure. **Figure 2** shows a schematic drawing of the test setup components along with the key dimensions. A 5000 kN (1100 kip) hydraulic machine was used to apply a concentrated load centered over the midspan of each slab. The loads were transferred to the slabs via a single longitudinal rigid steel spreader beam, outfitted with web stiffeners for greater rigidity, and then through transverse supports attached to two transverse spreader beams, each of which provided a distributed line load along the full width of the slab. Plaster was used between the transverse spreader beams and the slab to fill any surface irregularities and to avoid premature localized bearing failure. Resting on the supports, the slabs had a centerline-to-centerline span of 4850 mm (191 in.), divided into a pure bending middle span and two outside shear spans. During testing, the monotonic load was applied at a stroke-controlled rate of 1.0 mm/min (0.04 in./min) until first cracking. After cracking, the rate was increased to 2.0 mm/min (0.08 in./min) until failure. Loading was interrupted intermittently, approximately every 20 kN (4.5 kip), to delineate cracks, take photographs, and record observations.

Deflection was monitored using linear variable displacement transducers, which were placed along the span length of each specimen to ensure that a deflection profile could be established. To record the tensile strains in the internal steel strands, eight 2 mm (0.08 in.) long electrical strain gauges were installed along the longitudinal axis of the prestressed strands. In addition, 6 mm (0.2 in.) long electrical strain gauges were installed to measure the tensile strain along the near-surface-mounted CFRP reinforcement in longitudinal and transverse directions. The instrumentation layout was the same for the steel and CFRP reinforcement. In addition, either a single 50 mm (2 in.) electrical strain gauge or a PI gauge was installed in the middle of the slab's side face 10 mm (0.4 in.) from the slab top surface to measure the concrete compressive strain. A PI gauge was also installed in the middle of the side face of the slab at the location of the internal reinforcement, typically 45 mm

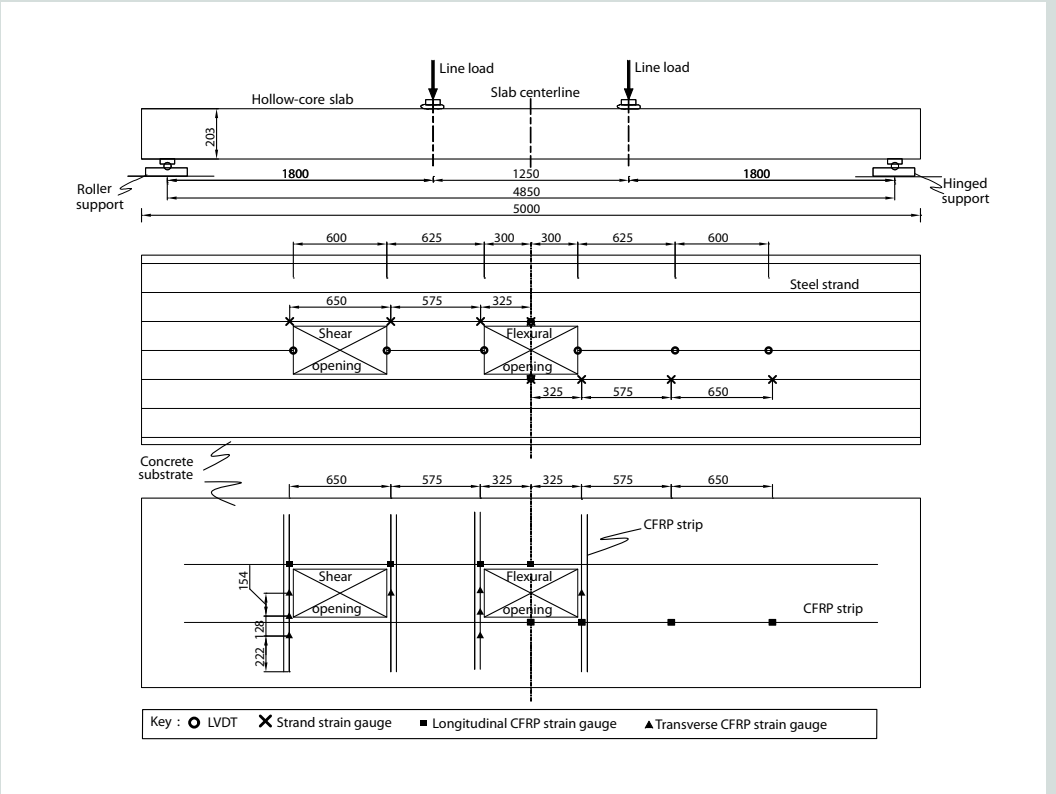

Figure 2. Test setup and instrumentation layout. Note: CFRP = carbon-fiber-reinforced polymer; LVDT = linear variable differential transformer. All dimensions are in millimeters. 1 mm = 0.0394 in.

(1.8 in.) from the slab soffit. A data acquisition system was used to collect readings from all sensors, including the applied load, deflection, compressive strains, and tensile strains in both sets of reinforcement. **Figure 2** illustrates the instrumentation employed to monitor the behavior of the specimens.

Test results and discussion

Cracking behavior

Figure 3 illustrates the crack patterns at failure of the test slabs. In general, the formation of cracks in all specimens followed a typical cracking pattern of a member subjected to four-point bending. In the reference specimen NO-O, cracking initiated with a single vertical flexural crack from the tension face of the member, close to the midspan of the constant moment region. Additional flexural cracks formed until the yielding stage. After yielding and as the applied load approached the ultimate stage, no new cracks developed, while existing cracks continued to widen and propagate vertically toward the neutral axis until failure. For specimen FO-O with an opening along the flexural span, cracking originated at the corners of the opening. Specimen SO-O with an opening along the shear span behaved similarly. After the initial cracks developed at the opening corners, the crack distribution developed similarly to the control specimen with no opening. Cracking was evenly distributed in the specimen with its opening centered at midspan and extended no farther than one slab depth beyond the loading points. When the opening was located along the shear span, cracking was limited to the side of the opening closest to the maximum moment region and to one slab depth beyond the loading points in the other side without opening. The majority of cracks initiating from the corners of the openings traveled in the transverse direction, directly toward the side of the slab. Near the failure of specimen SO-O, flexure-shear cracks formed in the shear span near the opening.

In specimens FO-S and SO-S, with longitudinal and transverse near-surface-mounted CFRP strips, cracks initiated simultaneously at the corners and perpendicular to the long sides of the openings. After reaching the yielding point, more cracks formed while the existing ones widened and propagated toward the compression zone. As the load increased, a significant number of minor cracks formed near the near-surface-mounted CFRP strips. The majority of these cracks were evenly distributed along the constant moment region. However, flexure-shear cracks were observed near the opening in slab SO-S.

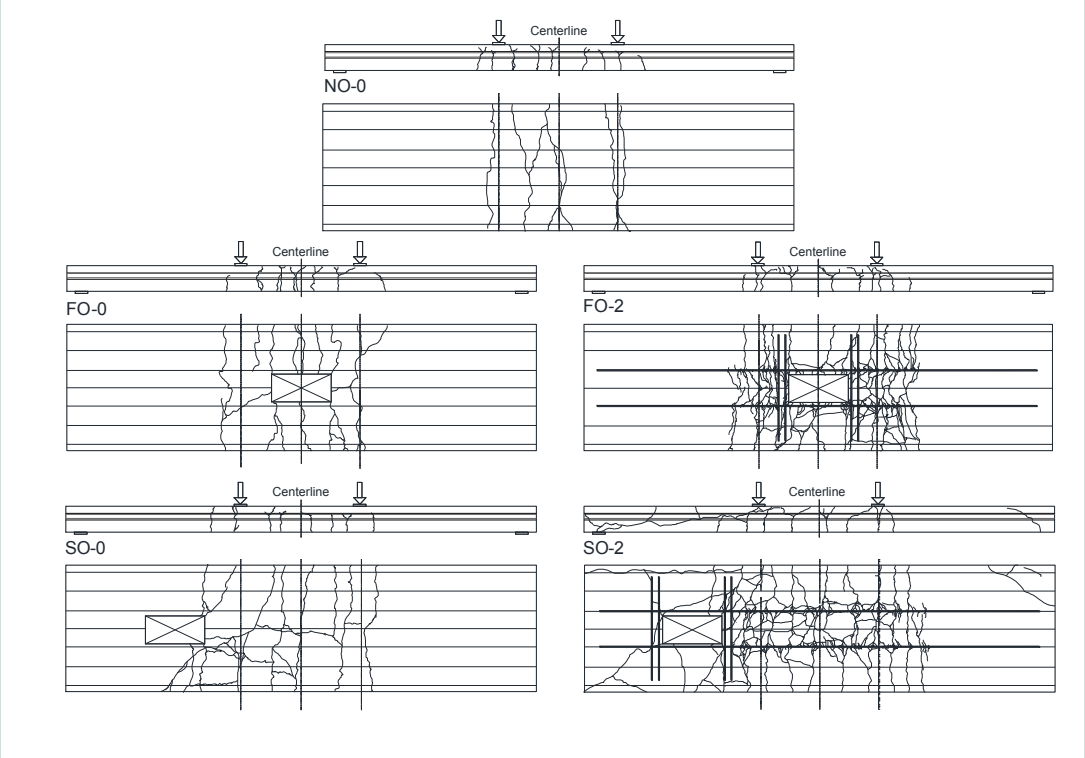

Figure 3. Cracking pattern at failure of test slabs. Note: CFRP = carbon-fiber-reinforced polymer; FO-O = slab with flexural span opening; FO-S = slab with flexural span opening strengthened with CFRP strips; NO-O = reference slab with no opening; SO-O = slab with shear span opening; SO-S = slab with shear span opening strengthened with CFRP strips.

Mode of failure

All tested slabs experienced steel yielding as the first stage of failure. Following steel yielding, specimens NO-O and FO-O failed due to concrete crushing and rupture of individual steel strands. After steel yielding, specimen SO-O experienced flexural-shear failure in the region between the loading point and the opening and finally by rupture of the strand running along the opening. Near failure in strengthened specimen FO-S, a pair of transverse strips delaminated from the concrete substrate. (Failure occurred in the surrounding concrete substrate as well as the surrounding adhesive matrix.) Afterward, the longitudinal strips experienced a partial delamination failure where several sections of the epoxy covering the longitudinal strips spalled off (adhesive cover spall) but did not fully debond from the substrate. This occurred within the maximum moment zone. Further increase in the load led the outermost tensile fibers of the CFRP strips to fray, essentially breaking away from the internal resin matrix. Finally, concrete crushing was observed at failure. Specimen SO-S demonstrated behavior similar to that of specimen SO-O, where a violent flexure-shear failure took place; however, delamination of the transverse and longitudinal CFRP strips was observed. Upon inspection of the near-surface-mounted system after failure, it was observed that the failure interface for the transverse strips was predominantly within the epoxy and did not extend into the surrounding concrete substrate. **Figure 4** shows photos of selected slabs at failure.

Deflection and ductility

Figure 5 shows the load-deflection relationship at the midspans of the test slabs. All test slabs demonstrated similar behavior that can be divided into precracking and postcracking stages. The precracking stage is characterized by a linear relationship and small deflections in all slabs. In the postcracking stage, excessive deformations can be seen, reflecting the reduced flexural stiffness after cracking. Slabs without strengthening showed large deformations without any significant increase in the load. The addition of

Concrete crushing in slab FO-O

Slab SO-O at failure

Slab FO-S at failure
and rupture of CFRP strip

Slab SO-S at failure

Figure 4. Photos for selected test specimens at failure. Note: CFRP = carbon-fiber-reinforced polymer.

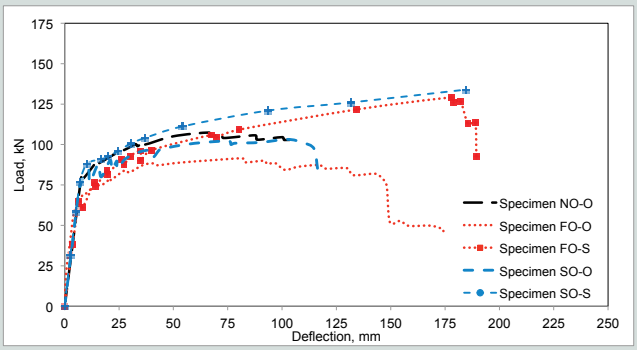

Figure 5. Load-deflection relationship at midspan of tested slabs. Note: CFRP = carbon-fiber-reinforced polymer; FO-O = slab with flexural span opening; FO-S = slab with flexural span opening strengthened with CFRP strips; NO-O = reference slab with no opening; SO-O = slab with shear span opening; SO-S = slab with shear span opening strengthened with CFRP strips. 1 mm = 0.0394 in.; 1 kN = 0.225 kip.

an opening within the slab reduced the postcracking flexural stiffness; however, the reduction in the postcracking stiffness due to an opening in the flexural zone was more significant than that due to an opening in the shear span. Strengthening the openings with near-surface-mounted CFRP strips improved the postcracking stiffness, as indicated by the steeper curve before failure. **Table 2** presents the postcracking stiffness calculated as the slope of the load-deflection curve. The postcracking stiffness decreased 56% and 43% in specimens FO-O and SO-O, respectively, compared with that of slab NO-O. However, the addition of the near-surface-mounted CFRP strips increased the postcracking stiffness 41% and 35% in specimens FO-S and SO-S, respectively, compared with their unstrengthened counterparts. Alternatively, the presence of the near-surface-mounted CFRP strips could not fully restore the original postcracking stiffness, where the postcracking stiffnesses in specimens FO-S and SO-S were 26% and 23% less than that of the reference specimen NO-O.

Table 2 provides a summary of the test results in terms of deflections at different loading stages and the corresponding calculated ductility for each slab. The ductility of the test slabs was analyzed in terms of deflection ductility μ_d and energy ductility μ_E. Deflection ductility is calculated as δ_u/δ_y, where δ_u and δ_y are the midspan deflections corresponding to the ultimate and yielding loads, respectively. Energy ductility is calculated based on a model developed by Oudah and El-Hacha.[16] In this model, energy ductility is defined as the ratio of the total energy (area under the load-deflection curve) and the elastic energy released at failure. The deflection at yielding and ultimate loads increased when adding the opening either in the flexural or shear spans. Consequently, these slabs exhibited higher deflection ductility and energy ductility compared with the reference slab. This could be attributed to the reduced flexural stiffness along the length of the slab. The deflection ductility of specimens FO-O and SO-O increased 4% and 42%, respectively, compared with that of specimen NO-O. The slight increase in the deflection ductility of specimen FO-O is due to its low capacity compared with specimen SO-O, which failed at a load similar to that of the control specimen. Similarly, energy ductility increased 42% and 85% in specimens FO-O and SO-O, respectively.

Table 2. Deflection and ductility results

Specimen	δ_{cr}, mm	δ_y, mm	δ_u, mm	Postcracking stiffness, N/mm	Deflection ductility		Energy ductility	
					μ_d	$\mu_d/\mu_{d(control)}$	μ_E	$\mu_E/\mu_{E(control)}$
NO-O	7.5	15.9	68.5	314.1	4.31	1.00	1.03	1.00
FO-O	8.2	19.1	85.4	137.0	4.47	1.04	1.46	1.42
FO-S	10.1	21.6	178.0	231.2	8.24	1.91	2.93	2.85
SO-O	6.8	17.8	108.6	177.8	6.10	1.42	1.82	1.77
SO-S	7.1	24.6	187.6	241.1	7.63	1.77	2.29	2.22

Note: CFRP = carbon-fiber-reinforced polymer; FO-O = slab with flexural span opening; FO-S = slab with flexural span opening strengthened with CFRP strips; f_{pu} = specified tensile strength of prestressed steel tendon; NO-O = reference slab with no opening; SO-O = slab with shear span opening; SO-S = slab with shear span opening strengthened with CFRP strips; δ_{cr} = midspan deflection at the estimated cracking stage; δ_u = midspan deflection corresponding to the ultimate load; δ_y = midspan deflection at $0.9f_{pu}$; μ_d = deflection ductility = δ_u/δ_y; $\mu_{d(control)}$ = deflection ductility of control specimens; μ_E = energy ductility; $\mu_{E(control)}$ = energy ductility of control specimens. 1 mm = 0.0394 in.; 1 N = 0.225 lb.

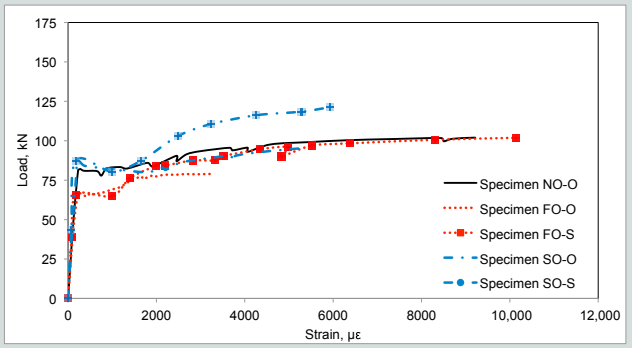

Figure 6. Load-strand strain relationship at midspan of tested slabs. Note: CFRP = carbon-fiber-reinforced polymer; FO-O = slab with flexural span opening; FO-S = slab with flexural span opening strengthened with CFRP strips; NO-O = reference slab with no opening; SO-O = slab with shear span opening; SO-S = slab with shear span opening strengthened with CFRP strips. 1 kN = 0.225 kip.

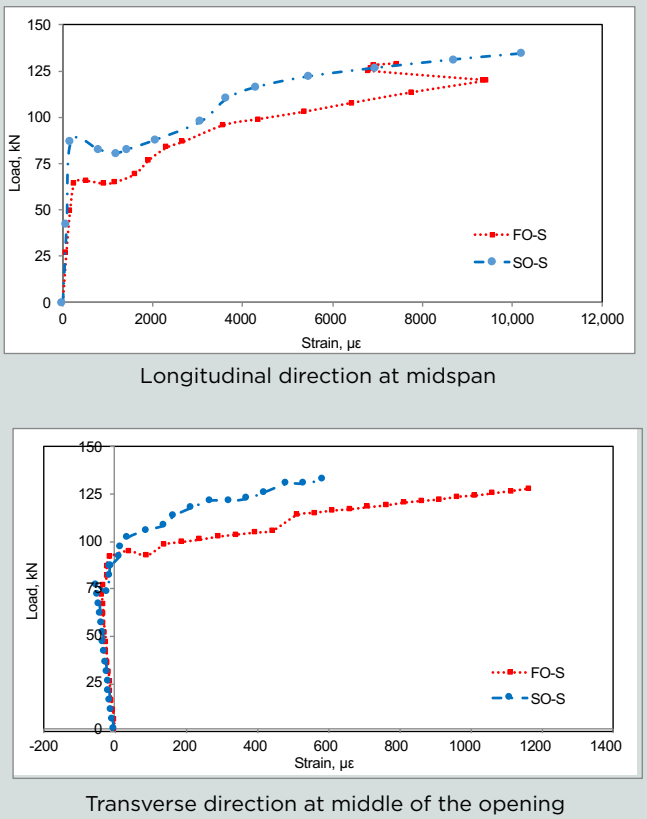

Figure 7. Load-strain relationship for near-surface-mounted CFRP strip. Note: CFRP = carbon-fiber-reinforced polymer; FO-S = slab with flexural span opening strengthened with CFRP strips; SO-S = slab with shear span opening strengthened with CFRP strips. 1 kN = 0.225 kip.

Slabs with strengthened openings also showed higher deflection ductility and energy ductility compared with that of the control specimen and their unstrengthened counterparts. However, this increase in ductility is mainly due to the higher ultimate capacities and the corresponding deflections of the strengthened slabs. Compared with reference specimen NO-O, the deflection ductility of specimens FO-S and SO-S increased 91% and 77%, which translates to 84% and 25%, respectively, compared with specimens FO-O and SO-O. Also, the increases in energy ductility were 185% and 122%, respectively, compared with the reference specimen. These increases in energy ductility are 200% and 25% higher than those of specimens FO-O and SO-O, respectively.

Strains

Figure 6 shows the load-strand strain relationship at midspan of all the test slabs. In the unstrengthened slabs, the strains in the strands were generally low up to the initiation of the cracks. The strains then increased rapidly until failure without significant increase in the load. In addition to the strain induced in the strands due to prestressing force, the measured strain at failure was approximately 9920×10^{-6} in specimen NO-O, while the strains in specimen FO-O, which failed at a lower load capacity, reached 3300×10^{-6} at approximately 90% of the ultimate load. At the corner of the opening in specimen FO-O, however, the measured strain in the strand reached approximately $11{,}120 \times 10^{-6}$. In specimen SO-O, the measured strain at midspan at 92% of the failure load was 5260×10^{-6}. Contrary to the unstrengthened slabs, the load-strain relationships in the slabs with strengthened openings were slightly different in that the strain kept increasing as the load increased up to failure. In specimens FO-S and SO-S, the strain gauges malfunctioned at approximately 78% and 90% of the ultimate load, respectively. At this load level, the strains were $10{,}130 \times 10^{-6}$ and 5940×10^{-6} in specimens FO-S and SO-S, respectively.

Figure 7 shows the relationship between the load and the measured strain in the longitudinal CFRP strips. The measured strains were insignificant before cracking of the slab; however, a considerable increase in strain was observed with increasing load, beyond cracking, until failure. Near failure, the measured strains at midspan were approximately 9370×10^{-6} and $10{,}210 \times 10^{-6}$ in specimens FO-S and SO-S, respectively. The transverse CFRP strips were not as effective as in the longitudinal direction, where the measured strains in CFRP strips were low until failure (Fig. 7). The maximum measured strains were 1170×10^{-6} and 590×10^{-6} in specimens FO-S and SO-S, respectively. This is mainly due to the formation of cracks parallel to the CFRP strips (Fig. 3).

Figure 8 shows the strain distribution along the longitudinal CFRP strip at different load levels for specimens FO-S and SO-S. In specimen FO-S, the strains

were symmetrical along the longitudinal CFRP strip, where the highest strains were measured in the opening zone and decreased toward the supports. This behavior was observed up to 90% of the ultimate load. The strain distribution along the slab was inconsistent due to the delamination of the CFRP strips in several locations, as discussed previously, at approximately 95% of the ultimate load. Similar behavior was observed for slab SO-S up to 90% of the ultimate load. However, once shear cracks formed near the opening (at approximately 95% of the failure load), the strain profile became unsymmetrical, with high strains observed in the opening side compared with those observed in the other side.

Experimental capacities of test slabs

Table 3 presents the cracking, yielding, and ultimate loads of the test specimens. The cracking load of the control specimen was approximately 81 kN (18 kip). In specimens FO-O and SO-O, the cracking loads decreased approximately 15% and 10%, respectively. In slabs with strengthened openings, the cracking load of specimen FO-S did not change and increased 5% in specimen SO-S compared with their unstrengthened counterparts. Regarding the load corresponding to yielding of strands, it was approximately 89.5 kN (20.1 kip) for the control specimen NO-O, while reductions of approximately 12% and 6% were observed in the yielding loads of specimens FO-O and SO-O, respectively. The addition of CFRP strips enhanced the yielding load by 8%, from 78.9 kN (17.7 kip) in specimen FO-O to 85.6 kN (19.2 kip) in specimen FO-S. However, the increase in yielding load was much higher for a slab with an opening in the shear span, where it increased from 84.4 kN (19.0 kip) in specimen SO-O to 94.7 kN (21.3 kip) in specimen SO-S.

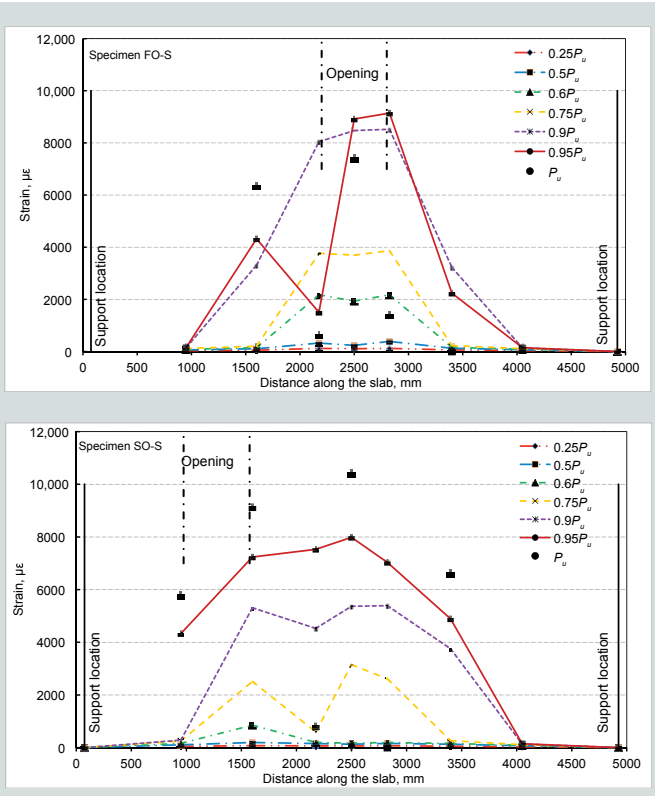

Figure 8. Strain distribution in near-surface-mounted CFRP strip in slabs FO-S and SO-S. Note: CFRP = carbon-fiber-reinforced polymer; FO-S = slab with flexural span opening strengthened with CFRP strips; P_u = experimental ultimate load; SO-S = slab with shear span opening strengthened with CFRP strips. 1 mm = 0.0394 in.

For the flexural test setup used in this study, compared with the control specimen, an opening along the flexural span decreased the ultimate capacity by 17%, while an opening along the shear span resulted in an insignificant decrease in the slab capacity of 4%. Alternatively, strengthening openings with near-surface-mounted CFRP strips effectively restored the flexural strength deficit incurred as a result of cutting the openings. The addition of strengthening reinforcement to a flexural opening and a shear opening resulted in significant capacity enhancements of 40% and 30%, respectively, compared with unstrengthened counterparts, which translates to net increases of 23% and 26%, respectively, compared with the reference specimen NO-O. This behavior indicates that the location of an opening has a significant effect on the cracking, yielding, and ultimate capacity of a prestressed hollow-core slab. Also, employing the near-surface-mounted strengthening technique is a suitable method to restore the capacity of the slab after adding openings.

Comparison between experimental and code-predicted capacities

The flexural capacity of the unstrengthened slab as well as the shear capacity of all slabs were calculated according to the Canadian standard CSA A23.3-14[17] and the American Concrete Institute's (ACI's) *Building Code Requirements for Structural Concrete (ACI 318-14) and Commentary (ACI 318R-14)*.[18] For strengthened slabs, CSA S806-12[19] specifies a maximum permissible strain in the near-surface-mounted reinforcement of 0.007, while ACI 440.2R-08[20] suggests a maximum permissible strain as a fraction of the ultimate tensile strain of the FRP reinforcement: 70% of the ultimate tensile capacity ($11{,}900 \times 10^{-6}$ for the used CFRP strips that have a mean rupture strain of $17{,}000 \times 10^{-6}$ as specified by the manufacturer). These codes provide no specific shear design provisions for members strengthened in flexure as is the case of the test slabs. **Table 3** summarizes the moment and shear capacities as determined using strain compatibility and the limits suggested by both design codes.

Table 3. Experimental test results and code predicted shear and flexural capacities

Specimen	P_{cr}, kN	P_y, kN	P_u, kN	Δ_{Pcr}, %	Δ_{Py}, %	Δ_{Pu}, %	Experimental		Predicted shear and flexural capacities			
									Canadian standards		American standards	
							V_{exp}, kN	M_{exp}, kN-m	V_{pred}, kN	M_{pred}, kN-m	V_{pred}, kN	M_{pred}, kN-m
NO-O	81	89.5	108	n/a	n/a	n/a	54	97	78.9*	103.3*	66.1†	108.6†
FO-O	69	78.9	92	-14.8	-11.8	-15.0	46	83	78.9*	81.0*	60.6†	91.0†
FO-S	70	85.6	129	-13.6 (1.4‡)	-4.4 (8.5‡)	19.4 (40‡)	64.5	116	78.9*	93.2§	56.9†	109.8‖
SO-O	73	84.4	103	-9.8	-5.6	-4.6	51.5	93	63.3*	94.6*	48.6†	105.2†
SO-S	77	94.7	134	-5.0 (5.5‡)	5.8 (12.2‡)	24.1 (30‡)	67	121	63.3*	106.2§	48.6†	125.5‖

Note: For SO-O and SO-S, the reported flexural capacities are calculated at midspan section while the shear capacities are calculated at the opening. CFRP = carbon-fiber-reinforced polymer; FO-O = slab with flexural span opening; FO-S = slab with flexural span opening strengthened with CFRP strips; M_{exp} = experimental bending moment; M_{pred} = predicted bending moment; n/a = not applicable; NO-O = reference slab with no opening; P_{cr} = experimental cracking load; P_u = experimental ultimate load; P_y = experimental yielding load; SO-O = slab with shear span opening; SO-S = slab with shear span opening strengthened with CFRP strips; V_{exp} = experimental shear force; V_{pred} = predicted shear force; Δ_{Pcr} = change in cracking load between strengthened and unstrengthened specimen; Δ_{Pu} = change in ultimate capacity between strengthened and unstrengthened specimen; Δ_{Py} = change in yielding load between strengthened and unstrengthened specimen. 1 kN = 0.225 kip; 1 kN-m = 0.738 kip-ft.

* Calculated according to CSA A23.3-14.

† Calculated according to ACI 318-14.

‡ Change in load compared with their unstrengthened counterparts.

§ Calculated according to CSA S806-12.

‖ Calculated according to ACI 440.2R-08.

In general, CSA A23.3-14[17] yielded good predictions of the flexural capacities of unstrengthened specimens (NO-O, FO-O, and SO-O) where the average experimental-to-predicted capacity was 0.98. ACI 318-14[18] slightly overestimated the capacity of the unstrengthened specimens, where the average experimental-to-predicted capacity was 0.9. However, better predictions were obtained for the strengthened specimens FO-S and SO-S, where the average experimental-to-predicted flexural strength ratios for the two specimens were 1.19 (CSA S806-12[19]) and 1.01 (ACI 440.2R-08[20]), respectively.

Conclusion

Based on the test results presented for a four-point bending setup, the following conclusions can be drawn:

- The presence of an opening in the flexural zone of prestressed hollow-core slabs decreased the cracking, yielding, and ultimate moment, while adding an opening in the shear span had less effect on the overall performance of such slabs.

- Strengthening openings with two strips of near-surface-mounted CFRP not only restored the flexural strength deficit incurred as a result of cutting the openings and the prestressing strand but provided additional flexural capacity.

- The postcracking stiffness of the slab decreased significantly (56%) with the addition of an opening in the constant moment region. Also, the addition of an opening in the shear span resulted in a 43% decrease in the postcracking stiffness. However, strengthening these openings with near-surface-mounted CFRP strips enhanced the postcracking stiffness, which increased 46% and 35% in specimens FO-S and SO-S, respectively, compared with their unstrengthened counterparts.

- Compared with the reference slab, slabs with openings exhibited higher deflection ductility and energy ductility, which could be attributed to reduced flexural stiffness after cutting the opening. Strengthened slabs showed higher ductility than their unstrengthened counterparts; however, this increase in ductility is attributed to the higher ultimate loads and the corresponding deflections of the strengthened slabs.

- Both the Canadian and American standards used in this study yielded reasonable predictions of the flexural capacity of prestressed hollow-core slabs with openings,

either unstrengthened or strengthened, with near-surface-mounted CFRP strips.

Acknowledgments

The authors would like to thank the Canada Research Chair Program (CRC), Tetra Tech Inc., Lafarge Canada Inc., and Vector Construction Ltd. for their financial support and industry perspectives. The assistance received from the technical staff at McQuade Structures Laboratory is also acknowledged.

References

1. De Lorenzis, L., and A. Nanni. 2002. "Bond between Near-Surface Mounted Fiber-Reinforced Polymer Rods and Concrete in Structural Strengthening." *ACI Structural Journal* 99 (2): 123–132.

2. El-Hacha, R., and S. H. Rizkalla. 2004. "Near-Surface-Mounted Fiber-Reinforced Polymer Reinforcements for Flexural Strengthening of Concrete Structures." *ACI Structural Journal* 101 (5): 717–726.

3. Hassan, T. K., and S. H. Rizkalla. 2004. "Bond Mechanism of Near-Surface-Mounted Fiber-Reinforced Polymer Bars for Flexural Strengthening of Concrete Structures." *ACI Structural Journal* 101 (6): 830–839.

4. Teng, J. G., L. De Lorenzis, B. Wang, R. Li, T. N. Wong, and L. Lam. 2006. "Debonding Failures of RC Beams Strengthened with Near Surface Mounted CFRP Strips." *Journal of Composites for Construction* 10 (2): 92–105.

5. De Lorenzis, L., and J. G. Teng. 2006. "Near-Surface Mounted FRP Reinforcement: An Emerging Technique for Strengthening Structures." *Composites Part B: Engineering* 38 (2): 119–143.

6. Yost, J. R., S. P. Gross, D. W. Dinehart, and J. J. Mildenberg. 2007. "Flexural Behavior of Concrete Beams Strengthened with Near-Surface-Mounted CFRP Strips." *ACI Structural Journal* 104 (4): 430–437.

7. Hajihashemi, A., D. Mostofinejad, and M. Azhari. 2011. "Investigation of RC Beams Strengthened with Prestressed NSM CFRP Laminates." *Journal of Composites for Construction* 15 (6): 887–895.

8. Badawi, M., and K. Soudki. 2009. "Flexural Strengthening of RC Beams with Prestressed NSM CFRP Rods—Experimental and Analytical Investigation." *Construction and Building Materials* 23 (10): 3292–3300.

9. Bencardino, F., G. Spadea, and R. N. Swamy. 2002. "Strength and Ductility of Reinforced Concrete Beams Externally Reinforced with Carbon Fiber Fabric." *ACI Structural Journal* 99 (2): 163–171.

10. Bonaldo, E., J. A. O. De Barros, and P. B. Lourenco. 2008. "Efficient Strengthening Technique to Increase the Flexural Resistance of Existing RC Slabs." *Journal of Composites for Construction* 12 (2): 149–159.

11. Enochsson, O., J. Lundqvist, B. Taljsen, P. Rusinowski, and T. Olofsson. 2007. "CFRP Strengthened Openings in Two-Way Concrete Slabs—An Experimental and Numerical Study." *Construction and Building Materials* 21 (4): 810–826.

12. Seliem, H., R. Seracino, E. Sumner, and S. Smith. 2011. "Case Study on the Restoration of Flexural Capacity of Continuous One-Way RC Slabs with Cutouts." *Journal of Composites for Construction* 15 (6): 992–998.

13. Smith, S., and S. J. Kim. 2009. "Strengthening of One-Way Spanning RC Slabs with Cutouts using FRP Composites." *Construction and Building Materials* 23 (4): 1578–1590.

14. Tan, K. H., and H. Zhao. 2004. "Strengthening of Openings in One-Way Reinforced-Concrete Slabs Using Carbon Fiber-Reinforced Polymer Systems." *Journal of Composites for Construction* 8 (5): 393–402.

15. CPCI (Canadian Precast/Prestressed Concrete Institute). 2007. *CPCI Design Manual*. 4th ed. Ottawa, ON, Canada: CPCI.

16. Oudah, F., and R. El-Hacha. 2012. "A New Ductility Model of Reinforced Concrete Beams Strengthened Using Fiber Reinforced Polymer Reinforcement." *Composites Part B: Engineering* 43 (8): 3338–3347.

17. CSA (Canadian Standards Association). 2014. *Code for the Design of Concrete Structures for Buildings*. CSA A23.3-14. Rexdale, ON, Canada: CSA.

18. ACI (American Concrete Institute) Committee 318. 2014. *Building Code Requirements for Reinforced Concrete (ACI 318-14) and Commentary (ACI 318R-14)*. Farmington Hills, MI: ACI.

19. CSA. 2012. *Design and Construction of Building Components with Fiber-Reinforced Polymers*. CAN/CSA-S806-12. Toronto, ON, Canada: CSA.

20. ACI Committee 440. 2008. *Guide for the Design and Construction of Externally Bonded FRP Systems for Strengthening Concrete Structures*. ACI 440.2R-08. Farmington Hills, MI: ACI.

Notation

b = width of the hollow-core slab element

f_{pu} = specified tensile strength of prestressed steel tendon

f_{py} = specified yield strength of prestressed steel tendon = $0.90f_{pu}$ for low-relaxation strands

M_{exp} = experimental bending moment

M_{pred} = predicted bending moment

P_{cr} = experimental cracking load

P_u = experimental ultimate load

P_y = experimental yielding load

V_{exp} = experimental shear force

V_{pred} = predicted shear force

δ_{cr} = midspan deflection at the estimated cracking stage

δ_u = midspan deflection corresponding to the ultimate load

δ_y = midspan deflection at $0.90f_{pu}$

Δ_{Pcr} = change in cracking load between strengthened and unstrengthened specimen

Δ_{Pu} = change in ultimate capacity between strengthened and unstrengthened specimen

Δ_{Py} = change in yielding load between strengthened and unstrengthened specimen

μ_d = deflection ductility

$\mu_{d(control)}$ = deflection ductility of control specimens

μ_E = energy ductility

$\mu_{E(control)}$ = energy ductility of control specimens

About the authors

Karam Mahmoud, PhD, is a postdoctoral fellow in the Department of Civil Engineering at the University of Manitoba in Winnipeg, MB, Canada.

Steven Foubert, MSc, PEng, is a project manager at Colliers Project Leaders in Winnipeg.

Ehab El-Salakawy, PhD, PEng, is a professor and Canada Research Chair in Durability and Modernization of Civil Structures in the Department of Civil Engineering at the University of Manitoba in Winnipeg.

Abstract

The effect of openings on the behavior of prestressed concrete hollow-core slabs and the efficiency of near-surface-mounted reinforcement as a strengthening technique are investigated. Five full-scale prestressed concrete hollow-core slabs were tested: one with no opening, two with openings in different locations, and two with identical openings strengthened with near-surface-mounted carbon-fiber-reinforced polymer (CFRP) strips. The slabs were tested in four-point bending. The openings were cut either in the pure flexural span or in the shear span. Test results showed that the presence of an opening along the flexure span or the shear span significantly decreased the postcracking flexural stiffness and capacity of the slab. In addition, strengthening openings with near-surface-mounted CFRP strips effectively enhanced the postcracking stiffness, increased the ductility of the member, restored the flexural strength deficit incurred as a result of cutting the openings, and provided a net increase in flexural capacity.

Keywords

Carbon-fiber-reinforced polymer strip, CFRP, ductility, hollow-core, parking structure, prestressing, reinforcement, roof.

Review policy

This paper was reviewed in accordance with the Precast/Prestressed Concrete Institute's peer-review process.

Reader comments

Please address reader comments to journal@pci.org or Precast/Prestressed Concrete Institute, c/o *PCI Journal*, 200 W. Adams St., Suite 2100, Chicago, IL 60606.